EPJ Web of Conferences **151**, 03001 (2017) DOI: 10.1051/epjconf/201715103001
LAM-16

Orbital free ab initio study of static and dynamic properties of some liquid transition metals

G. M. Bhuiyan[1,*], *Mohammad Riazuddin* Molla[1,2,**], *A. Z. Ziauddin* Ahmed[1,***], *L. E.* Gonzalez[3], and *D. J.* Gonzalez[3]

[1]Department of Theoretical Physics, University of Dhaka, Dhaka
[2]Department of Mathematics, University of Dhaka, Dhaka
[3]Departamento de Física Teórica, Universidad de Valladolid, Valladolid, Spain

Abstract. Several static and dynamic properties of liquid transition metals Cr, Mn and Co are studied for the first time using the orbital free ab-initio molecular dynamics simulation (OF-AIMD). This method is based on the density functional theory (DFT) which accounts for the electronic energy of the system whereas the interionic forces are derived from the electronic energy via the Hellman-Feynman theorem. The external energy functional is treated with a local pseudopotential. Results are reported for static structure factors, isothermal compressibility, diffusion coefficients, sound velocity and viscosity and comparison is performed with the available experimental data and other theoretical calculations.

1 Introduction

We have studied some static and dynamic properties of three liquid transition metals namely, *l*-Cr, *l*-Mn and *l*-Co by using the Orbital Free Ab-initio Molecular Dynamics (OF-AIMD) simulation method. These elements are lying in the middle of the 3*d* series and share some common features with the other transition metals. For example, they show strong *d*-band scattering and *sp*-*d* hybridization effect. The *d*-electrons are neither completely free to be treated by the extended band approach nor tightly bound to use the tight binding theory. In addition, physical properties of transition metals lying in the middle of the transition series are strongly affected by the interplay between the bonding and antibonding states [1, 2]. Glasses based on transition metals, being strong, are used in modern technological development. In order to understand physical properties of glasses, in particular the glass transition temperature, we often require the knowledge of diffusion coefficient, *D*, in the liquid phase. Because of the high melting temperatures of *l*-Cr, *l*-Mn and *l*-Co, the measurement of their diffusion coefficients is very difficult and, in fact, no experimental data for *D* are available for these liquid metals. So, in order to study the static and dynamic properties of the aforesaid metals a very useful option is computer simulation. For the last three decades, computer simulation has been a powerful tool to study different properties of condensed matter. Most ab-initio molecular dynamics simulation methods (AIMD) are based on density functional theory (DFT) [3, 4].

*e-mail: gbhuiyan@du.ac.bd
**e-mail: mriazmath@gmail.com
***e-mail: abuzafur@yahoo.com

Although the AIMD methods based on Kohn-Sham orbital version of DFT (KS-AIMD methods) are, in principle, more accurate, however, they imply heavy computational demands that limit both the size of simulation box and the simulation time. This limitation becomes worse if *d*-electrons are included in the calculation. However, some of the above problems can be partly alleviated by employing the Hohenberg-Kohn (orbital-free) version of the DFT (OF-AIMD method). The OF-AIMD simulation method allows to simulate larger systems, up to a few thousand particles. So, for our metals lying in the middle of the *3d*-series the application of OF-AIMD is quite justificatory. We stress that, to our knowledge, this is the first AIMD simulation study for *l*-Cr, *l*-Mn and *l*-Co.

The layout of this report is the following. Section 2 is devoted to the theories relevant to the OF-AIMD study for static and dynamic properties. We present results and discussion in section 3. This article is concluded in section 4.

2 Theory

The liquid metal is modelled as a set of N ions, each of valence Z, enclosed in a volume V, and interacting with $N_e = NZ$ electrons through an effective potential $v(r)$. According to DFT, the ground state electronic energy functional can be written as [3, 4]

$$E[n(\vec{r})] = T_s[n(\vec{r})] + E_H[n(\vec{r})] + E_{\rm xc}[n(\vec{r})] + E_{\rm ext}[n(\vec{r})] \tag{1}$$

where $T_s[n]$, $E_{\rm H}[n]$, $E_{\rm xc}[n]$ and $E_{\rm ext}[n]$ represent the electronic kinetic energy of non-interacting electrons, the Hartree energy, the exchange-correlation energy and the energy of interaction with the external potential, respectively. Additional details can be found in Refs. [5, 6]. The electronic exchange-correlation energy functional is treated with the local density approximation (LDA). As $E_{\rm ext}[n] = \int d\vec{r}\, n(\vec{r})\, v_{ext}(r)$, the external potential is modelled by a local ionic pseudopotential, $v_{ps}(r)$ [6]. The $v_{ps}(r)$ (see Ref. 5) has some parameters, (A, R_C and a), which have been chosen so that the OF-AIMD simulation reproduces the experimental static structure factors. To include the *sd*-hybridization effects we follow Wills and Harrison [7] and choose effective valence $Z = 1.5$ for all systems. More specifically we have used the following values for A, R_c and a (in atomic units): 0.050, 1.37, 0.65 (*l*-Cr), 0.005, 1.40, 0.75 (*l*-Mn) and 0.005, 1.39, 0.85 (*l*-Co) respectively.

3 Results and Discussions

The OF-AIMD simulation was performed by using 500 particles in a cubic simulation cell whose size was chosen to reproduce the experimental ionic number density. Given the ionic positions at time t, the energy functional is minimized with respect to the total electron density represented as $n(\vec{r}) = |\psi(\vec{r})|^2$, where $\psi(\vec{r})$ stands for an effective orbital. This is expanded in a plane wave basis set whose cutoff energies $E_{\rm cut} = 14$, 11, 14 Ryd were found adequate for *l*-Cr, *l*-Mn, and *l*-Co, respectively. Forces on the ions are derived from Hellmann-Feynman theorem. The ionic positions and velocities are updated by solving the Newton's equation of motion where the Verlet leapfrog algorithm is used with a time step of 7.6×10^{-3} ps for the three systems.

3.1 Static Properties

Figure 1(a) shows the form factor of non-Coulombic part of the v_{ps} for *l*-Cr, *l*-Mn and *l*-Co. It has the largest value at $q \to 0$ and quicky decreases before exhibiting a weak oscillatory behavior. The simulation allows a direct computation of both $S(q)$ and $g(r)$, and figure 1(b)

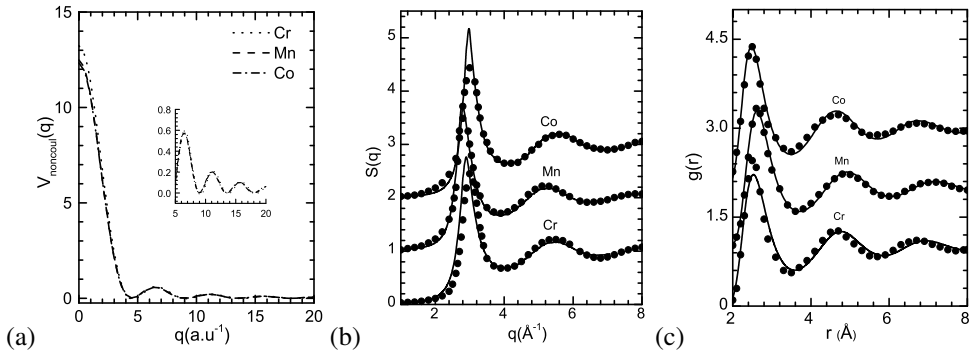

Figure 1. (a) Non-Coulombic potential, (b) static structure factor, $S(q)$ and (c) pair correlation function, $g(r)$, for l-Cr, l-Mn and l-Co at 2173, 1533 and 1823 K, respectively. The solid lines stand for OF-AIMD results and the closed circles for XR diffraction data.

shows the obtained $S(q)$ along with the respective x-ray data [8] for l-Cr, l-Mn and l-Co at T= 2173, 1533 and 1823 K, respectively. The main peak is overestimated in all cases but its position at q_p = 2.90, 2.76 and 2.97 Å^{-1} agrees with experiment. The positions and amplitudes of the subsequent peaks show a reasonable agreement with the respective experimental data. In the long wavelength limit the static structure factor is connected to thermodynamics via the relation $S(q \to 0) = \rho k_B T \chi_T$, where χ_T, ρ, k_B and T denote the isothermal compressibility, the average ionic number density, Boltzmann's constant and temperature, respectively. We have estimated $S(q \to 0)$ by fitting our calculated $S(q)$ with a quadratic function, within the range $q < 0.7$Å^{-1}, and we found χ_T = 0.79±0.01, 1.27±0.03 and 0.69±0.01 (in 10^{-12}cm^2 dyne^{-1} units) for l-Cr, l-Mn and l-Co, respectively. Values of χ_T, in the same units, for the corresponding solid phase at room temperature are 0.60, 0.83 and 0.55, respectively. The enhancement of compressiblity in the liquid phase near melting temperature is found to be 30% to 40% larger than parent solids. To our knowledge, no experimental data are available for the liquid phase, but an estimation from the low-q experimental $S(q)$ values of Waseda [8] has yielded $\chi_T \approx$ 0.82, 1.73 and 0.89 (same units) for l-Cr, l-Mn and l-Co, respectively. The pair correlation function $g(r)$ provides information about the short range order in the liquid state. Figure 1(c) depicts our calculated $g(r)$ for l-Cr, l-Mn and l-Co and they are compared with the x-ray data of Waseda [8]. We observe an overall agreement for the positions and amplitudes of the peaks. The coordination numbers were obtained by integrating $4\pi r^2 \rho\, g(r)$ up to the first minimum of the pair distribution function and the obatined results were 12.08, 12 and 12.43 for l-Cr, l-Mn and l-Co respectively. For comparison, we note that a similar calculation using the experimental pair distribution functions [8] yielded 11.68, 11.69, 11.75 for l-Cr, l-Mn and l-Co, respectively.

3.2 Dynamic properties: Single Particle Dynamics

The self-intermediate scattering function

$$F_s(q,t) = \frac{1}{N}\langle \sum_{j=1}^{N} \exp[i\vec{q}\cdot\vec{R}_j(t+t_0)] \exp[-i\vec{q}\cdot\vec{R}_j(t_0)\rangle, \tag{2}$$

provides information about the single particle dynamics over different length scales going from hydrodynamic ($q \to 0$) to free particle ($q \to \infty$) limit. Here $\langle ... \rangle$ denotes the average

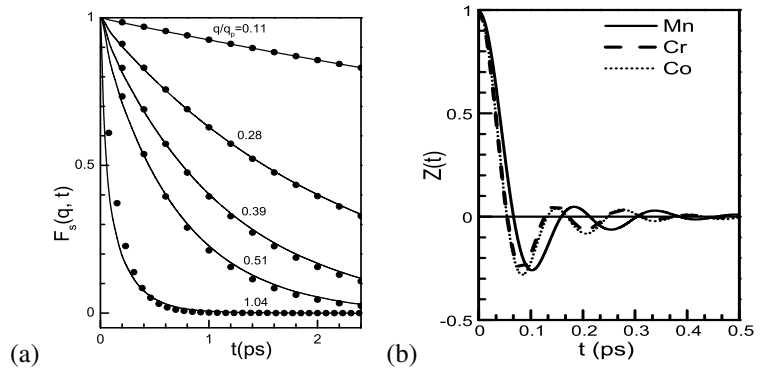

Figure 2. (a) $F_s(q,t)$ of l-Cr for several q. Full lines: OF-AIMD results. Full circles: Gaussian approximation (b) Normalized velocity autocorrelation functions of l-Cr , l-Mn, and l-Co.

over time origin and wave vectors with the same modulus. The velocity autocorrelation function (VACF) of a tagged ion in the fluid, $Z(t)$, is related to the time derivative of $F_s(q,t)$ in the hydrodynamic limit [9] but we have evaluated it from its definition

$$Z(t) = \langle \vec{v}_1(t)\vec{v}_1(0)\rangle / \langle v_1^2\rangle. \tag{3}$$

The self diffusion coefficient, D, is related to the time integral of $Z(t)$ via the Green-Kubo relation

$$D = \frac{k_B T}{m} \int Z(t)dt. \tag{4}$$

It is interesting to note that, $F_s(q,t)$ may be expressed within the Gaussian approximation (GA) as $F_s(q,t) = \exp[-\frac{1}{6}q^2\delta R^2(t)]$, where $\delta R^2(t)$ stands for the mean square displacement. Figure 2(a) shows, for l-Cr, the calculated $F_s(q,t)$, for several values of q. and it is compared with the result from the Gaussian approximation. $F_s(q,t)$ displays the typical monotonic non-linear decrease with time which becomes faster with increasing q/q_p values; in fact this trend is similar to that of the simple liquid metals near their respective triple points. It is noticed from the figure that the GA completely merge with $F_s(q,t)$ for low q values, but deviates somewhat at small t and large q. This clearly reveals the shortcomings of the GA. We note here that similar features have also been observed for l-Mn and l-Co.

The velocity autocorrelation function, $Z(t)$, is depicted in figure 2(b) for l-Cr, l-Mn and l-Co. The negative value of $Z(t)$ indicates backscattering of ions due to cage effects produced by the shell formed by surrounding neighbours. The self-diffusion coefficient, D, has been calculated from $Z(t)$ and we have obtained D= 0.71 ± 0.01, 0.53 ± 0.01 and 0.41 ± 0.02 Å^2/ps for l-Cr, l-Mn and l-Co, respectively. To our knowledge, no experimental data are available, therefore we have compared with other theoretical estimates. The scaling law of Dzugutov yields a value of D=0.712 Å^2/ps for l-Cr. For l-Mn other calculations have yielded D= 0.52 [10] and 0.42 [11] whereas for l-Co another theoretical calculation obtained 0.41 Å^2/ps [12].

3.3 Dynamic properties: Collective dynamics

The intermediate scattering function, $F(q,t)$ (see Ref.11), provides information about the collective dynamics of density fluctuations and its time Fourier transform yields the dynamic

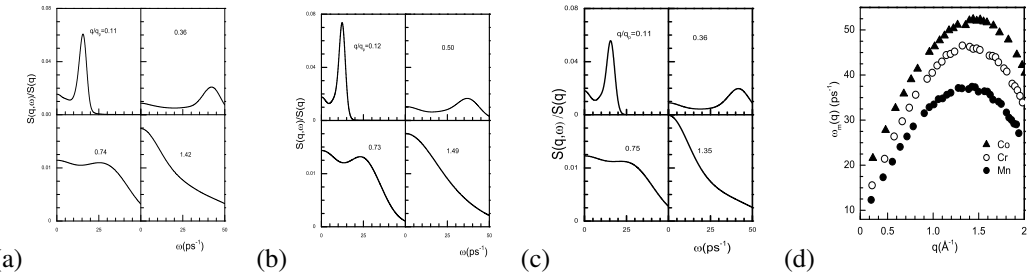

Figure 3. $S(q,\omega)$ for (a) *l*-Cr, (b) *l*-Mn, (c) *l*-Co and (d) their dispersion curves.

Table 1. Transport coefficients for *l*-Cr, *l*-Mn and *l*-Co.

Sys - tem	D(Å^2/ps)		c_S(m/s)		η(mPas)	
	OF-AIMD	Theo.	OF-AIMD	Exp.	OF-AIMD	Exp. (Theo.)
Cr	0.71	0.71	4586	4520	2.96	(2.96)
Mn	0.53	0.52, 0.42	3790	3710	2.74	(2.73)
Co	0.41	0.37, 0.41	4547	4090	4.15	4.1-5.3, 3.9

structure factor $S(q,\omega)$. Figures 2(a-c) show the calculated $S(q,\omega)$ for *l*-Cr, *l*-Mn and *l*-Co for several q values. It is noticed that up to $q/q_p \approx 0.73$, 0.77 and 0.75 (for *l*-Cr, *l*-Mn and *l*-Co, respectively) the obtained $S(q,\omega)$ exhibit well defined side peaks indicating the existence of collective density excitations. At $q/q_p > 0.73, 0.77$ and 0.75 a shoulder instead of a peak is observed first, and therefrom the $S(q,\omega)$ decrease monotonically. From the positions of the side peaks, $\omega_m(q)$, a dispersion relation of the density fluctuations has been obtained (see figure 3(d)). The slope of the dispersion curves evaluated at $q \to 0$ provides an estimation of adiabatic sound velocity c_s. It is interesting to note that c_s is connected to the ratio of specific heat γ which inturn is related to the Landau-Placzek ratio. The values of γ obtained from c_s are found to be 1.05, 1.09 and 1.09 for *l*-Cr, *l*-Mn and *l*-Co, respectively. Table 1 shows that the calculated c_s are in good agreement with the respective experimental values. Another interesting dynamical magnitude is provided by the current

$$\vec{j}(q,t) = \sum_{j=1}^{N} \vec{v}_j \exp[i\vec{q}\cdot\vec{R}_j(t)], \tag{5}$$

associated with the overall motion of the particles. This is usually split into a longitudinal component, $\vec{j}_l(q,t)$, parallel to $\vec{q}$ and, a transverse component, $\vec{j}_t(q,t)$, perpendicular to $\vec{q}$. The corresponding autocorrelation functions are the longitudinal, $C_l(q,t)$, and transverse, $C_t(q,t)$, correlation functions. $C_l(q,t)$ is basically the second time derivative of $F(q,t)$, and it does not bear any new physics. On the other hand, the transverse current correlation function $C_t(q,t)$ is related to the relaxation of shear stresses, and in the hydrodynamic limit yields the shear viscosity coefficient, η, through the memory function representation of $C_t(q,t)$. Values of the shear viscosity calculated for *l*-Cr, *l*-Mn and *l*-Co are presented in table 1 and we observe excellent agreement with experimental data [13] for *l*-Co. For *l*-Cr and *l*-Mn we are not aware of any experimental data, but other theoretical estimates are very close to the present ones.

4 Conclusion

Static and dynamic properties of *l*-Cr, *l*-Mn and *l*-Co transition metals near their respective triple points, have been studied near for the first time by using an AIMD simulation method. The calculated static structure agrees well with diffraction data and the calculated diffusion coefficients show a qualitative agreement with other theoretical estimates. Since experimental data for D do not exist, the present OF-AIMD values may be reliably used in other studies. The adiabatic sound velocity, c_S, obtained from our simulation data for *l*-Cr and *l*-Mn agree very well with experiment, but for *l*-Co agreement is not so good. In the case of shear viscosity, η, agreement between OF-AIMD and experiment is excellent for *l*-Co. Experimental data for η are not available for *l*-Cr and *l*-Mn , but other theoretical values are very close to ours. This agreement provides additional confidence on our obtained simulation values. Finally, we conclude that the OF-AIMD simulation method describes static and dynamic properties of liquid transion metals rather well and we expect that application of the KS-AIMD simulation method for these systems might improve results further.

GMB thanks AvH foundation for the grant subsidy to attend the LAM-16 conference, MRM acknowledges Ministry of Science and Technology, Bangladesh for fellowship under the project of Bangabandhu Fellowship on science and ICT, LEG and DJG acknowlegde the support of MECD (FIS2014-59279-P) and JCyL (VA104A11-2).

References

[1] K. A. Gschneider, Solid State Physics **16**, 275 (1974).
[2] J. Friedel, The physics of Metals 1. Electrons, ed. J.M. Ziman, Cambridge University Press(1971).
[3] P. Hohenberg, and W. Kohn, Phys. Rev. B **136**, 864 (1964).
[4] W. Kohn, and L. J. Sham, Phys. Rev. A **140**, 1133 (1965).
[5] G. M. Bhuiyan, L. E. González, and D. J. González, Cond. Matt. Phys. **15**, 33604, 1 (2012).
[6] G. M. Bhuiyan ,L. E. González, and D. J. González, Euro. Phys. J. Web of Conferences, **15**, 011011, (2011).
[7] J. M. Wills and W. A. Harrison, Phys. Rev. B,**28**,3199 (1988).
[8] Y. Waseda, The Structure of Non-Crystalline Materials. McGraw-Hill, New York, 1980.
[9] U. Balucani, and M. Zoppi, *Dynamics of the Liquid State*,Clarendon, Oxford, 1994.
[10] P. B. Thakor, Y. A. Sonvane, and A. R. Jani, AIP Conf. Proc. **1447**,915 (2012).
[11] R. C. Gosh, M. R. Amin, and G. M. Bhuiyan, J. Mole. liquids **188**,148 (2013).
[12] I. Yokoyama, Physica B **291**,145 (2000).
[13] G. Kaptay, Z. Metall.**1**,96 (2005); I. Egry, Scr. Metall. Mater. **28**,1273 (1993).